

# Integral Assessment of Gas Exchange During Venous-Arterial ECMO - Accuracy and Precision of a Modified Fick Principle in a Porcine Model

David Berger<sup>1</sup>, Lena Zwicker<sup>1</sup>, Kay Nettelbeck<sup>1,2</sup>, Daniela Casoni<sup>2</sup>, Paul Philipp Heinsch<sup>3</sup>, Hansjörg Jenni<sup>3</sup>, Matthias Haengggi<sup>1</sup>, Luciano Gattinoni<sup>5</sup>, Kaspar F. Bachmann<sup>1,4\*</sup>

1 Department of Intensive Care Medicine, Inselspital, Bern University Hospital, University of Bern, Bern, Switzerland

2 Experimental Surgery Facility (ESF), Department for BioMedical Research, Faculty of Medicine, University of Bern, Switzerland

3 Department of Congenital and Pediatric Heart Surgery, German Heart Center Munich, Technische Universität München, Munich, Germany

4 Department of Anesthesiology & Pain Medicine, Inselspital, Bern University Hospital, University of Bern, Bern, Switzerland

5 Department of Anesthesiology, Medical University of Göttingen, University Medical Center Göttingen, Göttingen, Germany

## \*Corresponding Author

Kaspar Felix Bachmann, MD

Department of Anesthesiology & Pain Medicine and Department of Intensive Care Medicine, Inselspital, Bern University Hospital, University of Bern, Bern, Switzerland  
kasparfelix.bachmann@gmail.com

**Prior Presentations:** Not applicable

**Total Word Count:** Abstract: 250; Introduction:315; Discussion:985

**Running Head:** Cardiac output measurement through gas exchange during V-A ECMO

**Sources of funding:** The study was supported by grants from the Stiftung für Forschung in Anästhesiologie und Intensivmedizin (No. 26/2018) awarded to Kaspar Bachmann and David Berger and from the Fondation Johanna Dormüller-Bol (No. 481) awarded to Kaspar Bachmann.

**Conflict of Interest:** The Department of Intensive Care Medicine has, or has had in the past, research contracts with Abionic SA, AVA AG, CSEM SA, Cube Dx GmbH, Cyto Sorbents Europe GmbH, Edwards Lifesciences LLC, GE Healthcare, ImaCor Inc., MedImmune LLC, Orion Corporation, and Phagenesis Ltd. and research and development/consulting contracts with Edwards Lifesciences LLC, Nestec SA, and Wyss Zurich. The money was paid into a departmental fund; no author received any

33 personal financial gain. Authors Bachmann, Berger and Gattinoni filed a patent (PCT/EP2020/060428)  
34 for the described method, which was not prolonged.

35 The Department of Intensive Care Medicine received unrestricted educational grants from the  
36 following organizations for organizing a quarterly postgraduate educational symposium, the Berner  
37 Forum for Intensive Care (*until 2015*): Abbott AG, Anandic Medical Systems, Astellas, AstraZeneca,  
38 Bard Medica SA, Baxter, B | Braun, CSL Behring, Covidien, Fresenius Kabi, GSK, Lilly, Maquet, MSD,  
39 Novartis, Nycomed, Orion Pharma, Pfizer, and Pierre Fabre Pharma AG (formerly known as  
40 RobaPharm).

41 The Department of Intensive Care Medicine has received unrestricted educational grants from the  
42 following organizations for organizing biannual postgraduate courses in the fields of critical care  
43 ultrasound, management of extracorporeal membrane oxygenation, and mechanical ventilation:  
44 Abbott AG, Anandic Medical Systems, Bard Medica SA., Bracco, Dräger Schweiz AG, Edwards  
45 Lifesciences AG, Fresenius Kabi (Schweiz) AG, Getinge Group Maquet AG, Hamilton Medical AG,  
46 Pierre Fabre Pharma AG (formerly known as RobaPharm), PanGas AG Healthcare, Pfizer AG, Orion  
47 Pharma, and Teleflex Medical GmbH.

48

49 **ABSTRACT**

50 Assessment of native cardiac output during extracorporeal circulation is challenging. We  
51 assessed a modified Fick principle under conditions such as deadspace and shunt in 13  
52 anesthetized swine undergoing centrally cannulated veno-arterial extracorporeal membrane  
53 oxygenation (V-A ECMO, 308 measurement periods) therapy. We assumed that the ratio of  
54 carbon dioxide elimination ( $\dot{V}CO_2$ ) or oxygen uptake ( $\dot{V}O_2$ ) between the membrane and  
55 native lung corresponds to the ratio of respective blood flows. Unequal ventilation/perfusion  
56 ( $\dot{V}/\dot{Q}$ ) ratios were corrected towards unity. Pulmonary blood flow was calculated and  
57 compared to an ultrasonic flow probe on the pulmonary artery with a bias of 99 mL/min (limits  
58 of agreement -542 to 741 mL/min) with blood content  $\dot{V}O_2$  and no-shunt, no-deadspace  
59 conditions, which showed good trending ability (least significant change from 82 to 129 mL).  
60 Shunt conditions led to underestimation of native pulmonary blood flow (bias -395, limits of  
61 agreement -1290 to 500 mL/min). Bias and trending further depended on the gas ( $O_2$ ,  $CO_2$ ),  
62 and measurement approach (blood content vs. gas phase). Measurements in the gas phase  
63 increased the bias (253 [LoA -1357 to 1863 mL/min] for expired  $\dot{V}O_2$  bias 482 [LoA -760 to  
64 1724 mL/min] for expired  $\dot{V}CO_2$ ) and could be improved by correction of  $\dot{V}/\dot{Q}$  inequalities. Our  
65 results show that common assumptions of the Fick principle in two competing circulations  
66 give results with adequate accuracy and may offer a clinically applicable tool. Precision  
67 depends on specific conditions. This highlights the complexity of gas exchange in membrane  
68 lungs and may further deepen the understanding of V-A ECMO.

69

## 70 INTRODUCTION

71 Venous-arterial extracorporeal membrane oxygenation (V-A ECMO) has been increasingly  
72 used as a rescue strategy in intensive care medicine for severe cardiopulmonary failure in  
73 the last decade (30). Particularly, the use of extracorporeal life support in the setting of  
74 cardiopulmonary resuscitation and post-cardiotomy cardiogenic shock are established  
75 concepts (1, 19). Mortality and morbidity with this treatment modality remain excessively high  
76 (up to 50%) (18, 20). Despite their paramount importance in guiding therapy, standard  
77 hemodynamic monitoring methods of the patient's conditions are influenced by the altered  
78 physiology on ECMO. It is increasingly recognized that standard methods for continuous  
79 cardiac output monitoring like trans-pulmonary thermodilution (15) or the pulmonary artery  
80 catheter lack validation (4, 31) and may therefore not serve their intended purpose during  
81 ECMO. Our study group has recently demonstrated that classic approaches of trans-cardiac  
82 thermodilution are not valid without conceptual adaptations in the setting of V-A ECMO (5).  
83 Echocardiography as a recommended tool remains non-continuous and user-dependent  
84 (31). The precise measurement and monitoring of native cardiac output was identified as an  
85 urgent clinical need (29).

86 Assessment of alveolar gas exchange is a traditional physiological method for measuring  
87 cardiac output, with various techniques (27). Expiratory gas measurements are readily  
88 available in intensive care and operating theaters. These may offer a new, standardized,  
89 non-invasive and continuous monitoring technique for cardiac output measurement in the  
90 context of ECMO. We have recently applied such methodology using a modified Fick  
91 principle and carbon dioxide measurements in a proof-of-concept animal model of V-A  
92 ECMO with specific adaptations regarding the extracorporeal component under healthy  
93 conditions (3). In an in-vitro model, we showed that this modified Fick approach based on  
94 oxygen blood content measurements allows calculation of cardiac output with a very small  
95 bias (4).

96 To assess measurements of native cardiac output through gas exchange parameters during  
97 V-A ECMO further, this current study addresses this research question in a large sample of  
98 animals in a well-controlled experimental setting and defines the critical steps for the  
99 development of a method usable at the bedside. First, we determined the performance of the  
100 modified Fick approach based on blood content measurements, including baseline, dead  
101 space, and shunt conditions. This assessed the performance under common  
102 pathophysiological states affecting the gas exchange. Second, in order to enable continuous  
103 measurements of cardiac output at the bedside, we assessed the performance of the  
104 modified Fick principle in the gas phase. Therefore, we compared calculations for blood  
105 content and gas content for respiratory gas measurements and the respective effects on the

106 performance of the cardiac output calculations. This stepwise approach enabled us to  
107 describe the inherent physiological limitations of our modified Fick technique, the limitations  
108 in measurement techniques, and the resulting relationship between gaseous measurements  
109 of oxygen and carbon dioxide and measurements in the blood phase. Finally, our extensive  
110 data set has enabled the description of in vivo extracorporeal gas exchange, providing real-  
111 life insights into gas exchange during V-A ECMO therapy that is comparable to mathematical  
112 models.

## 113 METHODS

114 The Commission of Animal Experimentation of Canton Bern, Switzerland, approved this  
115 study (BE111/18) in compliance with Swiss national guidelines and the *Guide for the Care*  
116 *and Use of Laboratory Animals* (National Academy of Sciences, 1996). This report follows  
117 the applicable ARRIVE (animal research: reporting of in vivo experiments) guidelines. The  
118 data that support the findings of this study are available from the corresponding author upon  
119 reasonable request. Data from this study on an adapted thermodilution technique have been  
120 published separately (5).

## 121 ANESTHESIA AND SURGERY

122 After premedication with ketamine, 16 healthy pigs ("Schweizer Edelschwein," *Sus scrofa*,  
123 45.5 kg, [42–47 kg], 10 females) were anesthetized and ventilated (Hamilton C6, volume  
124 control mode, positive end-expiratory pressure 5 cm H<sub>2</sub>O, F<sub>I</sub>O<sub>2</sub> 0.6). The animals underwent  
125 central V-A ECMO cannulation after sternotomy and heparinization (Figure 1A). The details  
126 of animal care and the anesthesiologic and surgical management of this experiment have  
127 been previously published (5).

128 The right atrium and ascending aorta were cannulated (29 Fr 3-stage venous cannula MC2X  
129 and 18 Fr elongated one-piece arterial cannula, Medtronic, Minneapolis, Minnesota, USA)  
130 and connected to an ECMO circuit (Stöckert SCPC console, LivaNova, London, England and  
131 Revolution centrifugal blood pump, LivaNova, London, England with CAPIOX FX15  
132 oxygenator, Terumo, New Jersey, USA). Transit time ultrasonic flow probes (Transonic PAU  
133 series, Ithaca, New York, USA, size 20/18 mm and 8 mm) were mounted around the  
134 pulmonary artery main trunk and the left pulmonary artery and the ECMO return cannula  
135 (Transonic ME9PXL1507, Ithaca, New York, USA). A Fogarty balloon catheter was placed in  
136 the left pulmonary artery for intermittent partial occlusion. A 1-lumen central venous line was  
137 placed in the left atrium for pressure measurement. Another 1-lumen catheter line was  
138 inserted surgically in the right ventricle. Temperature was kept at 37.0 °C using a  
139 temperature control system (HCV, Type 20–602, Jostra Fumedica, Muri, Switzerland).

140 Sweep gas was blended from air and oxygen with two respective mass flow controllers  
141 (Vögtlin RED-Y, Basel-Land, Switzerland) to achieve a constant inlet oxygen concentration  
142 (F<sub>d</sub>O<sub>2</sub>) of 0.6. Sweep gas flow was always set to match blood flow at the ECMO (resulting in  
143 a ventilation/perfusion [ $\dot{V}/\dot{Q}_{ECMO}$ ] ratio of 1) with reductions in sweep gas flow only during  
144 stabilization periods between experimental maneuvers to achieve a pH of 7.4–7.5 (14).

## 145 EXPERIMENTAL PROTOCOL

146 After surgery, instrumentations were controlled using fluoroscopy. During a stabilization  
147 period of 60 min, all devices were calibrated and measurements initiated. The experimental  
148 protocol (Figure 1B) consisted of four phases: baseline, thermodilution, and shunt and dead

149 space in randomized order. The thermodilution phase has been analyzed and published  
150 separately (5) and is not discussed here. Dead space was created through intermittent  
151 inflation of the Fogarty balloon catheter in the left pulmonary artery, and shunt was achieved  
152 by selective intubation of the left main bronchus. The flow probe on the left pulmonary artery  
153 confirmed the effect of these maneuvers. The baseline, shunt, and dead space phases  
154 consisted of four ECMO blood flow reductions ranging from 4 L/min to 1 L/min (1-L/min  
155 steps). Sweep gas flow was set to match blood flow ( $\dot{V}/\dot{Q}_{\text{ECMO}} = 1$ ). After each such flow  
156 reduction, the animal was allowed to stabilize for 5 min before a measurement period of 3  
157 min (resulting in four measurement steps per phase). In that period, five blood gas samples  
158 were drawn and measurements of gas exchange at the ventilator and the ECMO were  
159 recorded (see below). Each phase was repeated twice (i.e. baseline 1, baseline 2, shunt 1,  
160 shunt 2, deadspace 1, deadspace 2) with various ventilator settings to vary the  $\dot{V}/\dot{Q}$  ratio at  
161 the lung. For baseline 1 and 2 as well as deadspace 1 and 2, the ventilator was set to 10×10  
162 mL/kgBW (kilogram of body weight) and 15×10 mL/kgBW, respectively. For shunt 1 and 2,  
163 the ventilator was set to 10×6 mL/kgBW and 20×6 mL/kgBW, respectively. The ratio of  
164 inspiratory to expiratory time was constant at 1:1.6.

165 At the end of the experiments, the animals were euthanized in deep anesthesia with an  
166 injection of one mmol/kg potassium chloride under monitoring of the electrocardiogram and  
167 electroencephalogram to ensure asystole and brain death.

## 168 BLOOD GAS MEASUREMENTS

169 Blood gas samples were collected simultaneously by two qualified intensive care nurses at  
170 five ports: at the pulmonary artery (PA), left atrium (LA), ECMO inlet/right atrium (RA), post  
171 oxygenator (PE), and aorta (AO; Figure 1A). The samples were sealed airtight and  
172 immediately cooled for analysis within minutes. Depending on the availability on a respective  
173 day, either the cobas b123 POC (Roche Diagnostics, Basel, Switzerland) or ABL90 FLEX  
174 (Radiometer Medical, Copenhagen, Denmark) blood gas analyzer was used for the following  
175 measurements: partial pressure of carbon dioxide ( $p\text{CO}_2$ ), partial pressure of oxygen ( $p\text{O}_2$ ),  
176 hematocrit (Hct), hemoglobin (Hb), oxygen saturation ( $s\text{O}_2$ ), pH, and standard bicarbonate.  
177 Both devices have an integrated CO-oxymeter for measurement of oxygen saturation with  
178 coefficients for human hemoglobin. Since significant inter-species differences exist for these  
179 coefficients, all  $s\text{O}_2$  values were corrected for pigs using Serianni's approach (28).

## 180 ASSESSMENT OF GAS EXCHANGE

181 Breath-by-breath  $\text{CO}_2$  measurements and pulmonary elimination of  $\text{CO}_2$  ( $\dot{V}\text{CO}_{2\text{Lung}}$ ) were  
182 performed using a Capnostat 5 capnograph (Hamilton Medical, Bonaduz, Switzerland) at the  
183 endotracheal tube. For  $\text{O}_2$  uptake in the lung ( $\dot{V}\text{O}_{2\text{Lung}}$ ), the delay in the side-stream  $\text{O}_2$  signal  
184 was time matched to the mainstream  $\text{CO}_2$  signal and then integrated with gas flow at the  
185 tracheal tube (34). At the ECMO circuit, a side-stream module for indirect calorimetry (E-

186 COVX, General Electric, Baden, Switzerland) for continuous measurement of membrane  
 187 lung exhaust gas was attached. In the gas phase,  $\dot{V}CO_2$  was measured by integrating tidal  
 188 gas flow with the mainstream capnography and sweep flow with the exhaust capnography  
 189 signal (33, 34). Haldane's transformation was used to calculate post-oxygenator gas flow as  
 190 follows (assuming a nitrogen concentration of 0.79 at the air-fed flow controller) (36):

$$N_2inflow = AirFlow_{Inlet} * NitrogenConcentration \quad (1)$$

$$TotalGasFlow_{outlet} = \frac{N_2inflow}{1 - F_{PE}O_2 - F_{PE}CO_2} \quad (2)$$

191

192 Calibrations were performed on 7 of 16 experimental days using predefined mixtures of  
 193  $CO_2/N_2/O_2$ .

## 194 DATA ACQUISITION

195 Measurements included sweep gas and blood flow at the ECMO, blood flow through the  
 196 lungs, airway pressures, tidal volumes and flow, pulmonary end-tidal oxygen and carbon  
 197 dioxide tension ( $etO_2$ ,  $etCO_2$ ), pressures from the carotid artery, right atrium, left atrium, and  
 198 pulmonary artery, body temperature, ECMO exhaust oxygen and carbon dioxide tensions,  
 199 and continuous oximetric mixed venous saturation (calibrated every 3 h). Three-minute  
 200 measurement intervals were used.

201 All data output from temperature probes, pressure transducers, and ultrasonic blood flow  
 202 probes were recorded at 100 Hz in Labview (National Instruments Corp., Austin, Texas,  
 203 USA) and Soleasy (Alea Solutions, Zürich, Switzerland). Data from the respirator were  
 204 recorded at 50 Hz using a dedicated recording device (Memory Box, Hamilton Medical,  
 205 Bonaduz, Switzerland).

## 206 FORMULAS AND CALCULATIONS

207 Mass balance demands that in a steady state, total carbon dioxide production ( $\dot{V}CO_2$ ) and  
 208 total oxygen consumption ( $\dot{V}O_2$ ) have to match the elimination of  $\dot{V}CO_2$  at the lung plus  
 209 ECMO and the oxygen uptake at the lung plus ECMO, respectively. Using the Fick principle,  
 210 Eq. 3A can be deducted (3), where  $c_{V-AO}$  refers to the veno-arterial content difference,  $c_{V-LA}$   
 211 refers to the content difference over the pulmonary circulation, and  $c_{V-PE}$  refers to the content  
 212 difference over the ECMO circuit.  $\dot{Q}$  is the blood flow. In theory,  $CO_2$  can be substituted for  
 213 any other gas that is in equilibrium (Eq. 3B):

$$\dot{Q}_{total} * \Delta c_{\bar{v}-AO}CO_2 = \dot{Q}_{Lung} * \Delta c_{\bar{v}-LA}CO_2 + \dot{Q}_{ECMO} * \Delta c_{\bar{v}-PE}CO_2 \quad (3A)$$

$$\dot{Q}_{total} * \Delta c_{\bar{v}-AO}O_2 = \dot{Q}_{Lung} * \Delta c_{\bar{v}-LA}O_2 + \dot{Q}_{ECMO} * \Delta c_{\bar{v}-PE}O_2 \quad (3B)$$



214 Rearrangement of Eq. 3A and B proposes a proportional relationship of oxygen  
 215 consumption/carbon dioxide elimination and respective blood flows under the assumption  
 216 that  $\dot{Q}_{total} = \dot{Q}_{Lung} + \dot{Q}_{ECMO}$ :

$$\dot{Q}_{Lung} = \dot{Q}_{ECMO} * \frac{(\Delta\bar{v}_{-PE}CO_2 - \Delta\bar{v}_{-AO}CO_2)}{(\Delta\bar{v}_{-AO}CO_2 - \Delta\bar{v}_{-LA}CO_2)} \quad (4)$$

217  $\dot{V}CO_2$  is the product of the differences in  $CO_2$  content times the blood flow and thus Eq. 4 can  
 218 be simplified using the following assumptions:  $\dot{V}CO_{2ECMO}$  is proportional to  $\Delta_{v-PE}CO_2$ ,  
 219  $\dot{V}CO_{2Lung}$  is proportional to  $\Delta_{v-LA}CO_2$ ,  $\dot{V}CO_{2Total}$  is proportional to  $\Delta_{v-AO}CO_2$ , and the total  
 220  $\dot{V}CO_2$  is the sum of  $\dot{V}CO_2$  at the ECMO and the lung. As production and elimination are  
 221 mathematical opposites, we use absolute values (3).

$$\Delta\dot{Q}_{Lung} = \dot{Q}_{ECMO} * \frac{|\dot{V}CO_{2Lung}|}{|\dot{V}CO_{2ECMO}|} \quad (5)$$

$$\Delta\dot{Q}_{Lung} = \dot{Q}_{ECMO} * \frac{|\dot{V}O_{2Lung}|}{|\dot{V}O_{2ECMO}|} \quad (6)$$

222 The original Fick principle leads to the assumption that Eqs. 5 and 6 also hold true for  
 223 oxygenation and  $O_2$  consumption ( $\dot{V}O_2$ , Eq. 4). The full derivation of these equations can be  
 224 found in Bachmann and colleagues. (3).

225 The method of Dash and Bassingwaithe was used to calculate blood  $CO_2$  content ( $cCO_2$ )  
 226 (11, 37). Oxygen content ( $cO_2$ ) was calculated using the standard formula (Eq. 7):

$$cO_2 = 1.36 * Hb * \frac{sO_2}{100} + 0.003 * pO_2 \quad (7)$$

227 In the blood phase,  $\dot{V}CO_2$  and  $\dot{V}O_2$  were calculated as the difference between arterial and  
 228 venous content times measured blood flow.

229  $\dot{V}CO_2$  is highly dependent on the  $\dot{V}/\dot{Q}$  ratio and is thus dependent not only on blood flow but  
 230 also on ventilation (2). This interferes with the precision of blood flow calculations, as the  
 231 constructed mass balance equation is only applicable if the inflow and outflow gas content of  
 232 both the ECMO and the lung are equal. To correct for this, an empirical approach for  
 233 normalizing  $\dot{V}CO_2$  at the lung was applied (3).

$$f(\dot{V}, \dot{Q}) = \frac{\dot{Q} * \left(\frac{\dot{V}}{\dot{Q}} + c\right)}{\dot{V} * (1 + c)} = \frac{\left(\frac{\dot{V}}{\dot{Q}} + c\right)}{(1 + c)} * \frac{1}{\frac{\dot{V}}{\dot{Q}}} \quad (8)$$

234 The constant  $c$  was calculated from a venous blood gas sample [ $c = \sigma_{CO_2} * R * T * (1 + K_c)$ ]  
 235 as a function of temperature  $T$ , pH ( $K_c$ ),  $CO_2$  solubility ( $\sigma_{CO_2}$ ), and the gas constant  $R$  (17). In

236 brief, this normalization allows calculation of  $\dot{V}CO_2$  that is dependent on blood flow only and  
237 independent of ventilation;  $\dot{V}CO_2$  is therefore normalized toward a  $\dot{V}/\dot{Q}$  ratio of 1. To estimate  
238  $\dot{V}/\dot{Q}$  at the lung, we used a previously described mass balance equation (35):

$$\frac{\dot{V}}{\dot{Q}} = \frac{F_I O_2 - F_E O_2}{c_v O_2 - c_a O_2} \quad (9)$$

239 Blood gas calculations were performed using either  $\dot{V}O_2$  calculated as the product of blood  
240 gas  $O_2$  content difference times blood flow ( $\dot{V}O_{2\text{ Blood}}$ ),  $\dot{V}O_2$  measured in the gas phase ( $\dot{V}O_{2\text{ Gas}}$ ),  
241  $\dot{V}CO_2$  measured in the gas phase ( $\dot{V}CO_{2\text{ Gas}}$ ), normalized  $\dot{V}CO_2$  in the gas phase ( $\dot{V}CO_{2\text{ Gas Norm}}$ ), or  
242  $\dot{V}CO_2$  in the blood phase ( $\dot{V}CO_{2\text{ Blood}}$ ). Calculated blood flows were compared to  
243 measured blood flows for each experimental phase separately.

244 Arterial and venous oxygen content ( $c_a O_2$ ,  $c_v O_2$ ) were calculated from the blood gas samples.  
245 A normalization at the ECMO was not applied, as  $\dot{V}/\dot{Q}$  was specifically chosen to be 1.

## 246 STATISTICAL ANALYSIS

247 Analyses were performed using Matlab R2021a (MathWorks, Natick, Massachusetts, USA)  
248 with an extension for Bland–Altman plots under creative commons license (26). Data are  
249 presented as means with standard deviations or as medians with interquartile ranges where  
250 appropriate. Method agreement was tested with linear regression (least squares method)  
251 and Bland–Altman analysis (6, 7). A two-tailed  $p$  value of  $< 0.05$  was considered statistically  
252 significant. The least significant change of a method was calculated according to standard  
253 methods (23). The relationship between  $\dot{V}CO_2$  and  $\dot{V}O_2$  and the underlying parameters  
254 (blood gas content and blood flow) were assessed using linear mixed-effect models and  
255 analysis of variance with Bonferroni correction, if necessary. Outliers were removed  
256 according to the following rules: calculated blood flow  $> 10$  L/min or negative calculated  
257 pulmonary blood flows. Sample size was calculated from data from pilot animals, which  
258 showed an increase in pulmonary blood flow of 1 L/min for each 1 L/min reduction in ECMO  
259 flow. To detect these changes appropriately with a precision error of  $< 30\%$ , we calculated a  
260 sample size of 10 animals. To compensate for an expected dropout rate of 20% and to  
261 establish the experimental setup in four pilot animals, the experiment was performed in 16  
262 animals.

263

## RESULTS

264

### 265 *Summary of experiments*

266 After exclusion of one dead space maneuver (animal 5, due to technical recording problems),  
267 data from 13 animals with 308 measurement periods were analyzed, resulting in a total of  
268 1540 blood gas samples (7 animals with Radiometer, 9 animals with the cobas). ECMO flow  
269 was within the targets set by the protocol. Blood flow through the lung increased from median  
270 values of 833 – 1216 (ECMO flow 4 L/min) to median values of 2257 – 2541 mL/min with  
271 ECMO flow reductions (1 L/min), depending on the experimental condition. With these flow  
272 changes,  $\dot{V}O_2$  and  $\dot{V}CO_2$  changed accordingly with increases in  $\dot{V}O_2$  &  $\dot{V}CO_2$  at the lung and  
273 decreases in  $\dot{V}O_2$  &  $\dot{V}CO_2$  at the ECMO (e-Table 1 in the online supplement). Total  $\dot{V}O_2$  was  
274 approximately 200 mL/min, which corresponds to physiological values for pigs (14). Total  
275  $\dot{V}CO_2$  at the initial ECMO flow of 4 L/min was around 250 mL/min, resulting in a respiratory  
276 exchange ratio of approximately 0.8. Total  $O_2$  consumption and  $CO_2$  removal did not remain  
277 constant throughout ECMO flow changes. While  $\dot{V}O_{2\text{ Total}}$  measured in the blood phase  
278 remained mostly unchanged, there was a decrease in  $CO_2$  removal ( $\dot{V}CO_{2\text{ Total}}$ ) through the  
279 decrease in ECMO blood flow (e-Figure 1 in the online supplement).

### 280 *Cardiac output estimates based on oxygen content*

281 The first step was to test the modified Fick approach with oxygen content measurements in  
282 blood ( $\dot{V}O_{2\text{ Blood}}$ , Figure 2A). The resulting cardiac output showed low bias with narrow limits  
283 of agreement for baseline (Bias 99 mL, LoA -542 mL to 741 mL) and dead space conditions  
284 (bias 84 mL, LoA -487 mL to 654 mL). Shunt conditions lead to considerable loss in precision  
285 and accuracy (bias -395 mL, LoA -1290mL to 500 mL). The trending ability of these cardiac  
286 output calculations (i.e. the accordance between calculated changes and measured changes  
287 in blood flow) was high (least significant changes from 82 to 129 mL, Figure 2B).

288 Since continuous measurements are not possible in the blood, measurements in the gas  
289 phase would be of interest. The relationship between  $\dot{V}O_2$  in expired or exhaust air and  $\dot{V}O_{2\text{ Blood}}$   
290 is accurate but lacks precision (ECMO data: bias 10 mL/min with limits of agreement of -  
291 50 to 70 mL/min; lung data: bias 9 mL/min with limits of agreement of -43 to 61 mL/min; e-  
292 Figure 2 A and B in the online supplement).

293 Cardiac output estimates based on oxygen uptake measurements in the gas phase ( $\dot{V}O_{2\text{ Gas}}$ ,  
294 Figure 2C) provide acceptable accuracy, but low precision (Baseline: bias 253 mL, LoA -  
295 1357mL to 1863 mL; Shunt: Bias -399 mL, LoA -1658 mL to 860 mL; Dead space: bias 74  
296 mL, LoA -1575 mL to 1673 mL), and low accordance rates for trending (40 to 49%, Figure  
297 2D).

### 298 *Cardiac output measurements based on carbon dioxide contents*

299  $\dot{V}CO_{2\text{Blood}}$  showed considerable deviation from  $\dot{V}CO_{2\text{gas}}$  (bias -100 mL/min , LoA -222 mL/min  
300 to 21 mL/min for ECMO data and bias -10 mL/min, LoA 97 mL/min to 77 mL/min for lung  
301 data, e-Figure 2 C and D in online supplement). We suspect that this lack of agreement lays  
302 in the blood content model used (11). Since at the bedside, the gas measurement would  
303 allow continuous information and if blood measurements were available, oxygen content may  
304 be used, we omit further use of blood flow calculations using blood measurements of  $CO_2$ .

305 Cardiac output estimates resulting from  $\dot{V}CO_{2\text{gas}}$  measurements at the lung showed  
306 considerable bias with wide limits of agreement for baseline (Bias 894 mL, LoA -385 mL to  
307 2173 mL) and dead space (bias 500 mL, LoA -786 mL to 1758 mL) and Shunt (bias -260 mL,  
308 LoA -1420mL to 901 mL). The trending ability of these cardiac output calculations was  
309 moderate (least significant changes from 165 mL to 1186 mL, Figure 3 A and B).

310 Empirical normalization for the  $\dot{V}CO_{2\text{Lung}}$  (3) decreased the bias and narrowed the limits of  
311 agreement for baseline (Bias 482 mL, LoA -760 mL to 1724 mL), dead space conditions  
312 (bias 66 mL, LoA -879 mL to 1011 mL) and shunt conditions (bias 601 mL, LoA -870 mL to  
313 2071 mL bias -260 mL, LoA -1420mL to 901 mL). Of note,  $\dot{V}CO_{2\text{Gas Norm}}$  showed increased  
314 accordance and trending ability compared to calculations through  $\dot{V}CO_{2\text{Gas}}$  and  $\dot{V}O_{2\text{Gas}}$   
315 (Figure 3 C and D).

### 316 *Isolating the limiting factors*

317 The inflow (venous) and outflow (arterial) conditions between ECMO and lung were  
318 inhomogeneous. Venous oxygen saturations and  $pCO_2$  values differed substantially between  
319 ECMO drainage (right atrium) and the pulmonary artery (Figures 4 and 5, panels A and B).  
320 The difference in outflow saturations is relevant only for the shunt condition, where, as  
321 consequence of the experimental condition, saturations below 100% for left atrial blood  
322 occurred (Figure 4 B). The differences in arterial  $pCO_2$  values are a direct result of the  $\dot{V}/\dot{Q}$   
323 ratios being unequal to 1 at the lung (Figure 5 B).

324 Using linear-mixed effect models, the factors influencing these wide limits of agreement and  
325 bias were assessed. The models show a significant relationship between gaseous  
326 measurements and blood content difference and blood flow. The relationship differs  
327 depending on the measurement technique.  $\dot{V}CO_{2\text{Gas Norm}}$  and  $\dot{V}CO_{2\text{Gas ECMO}}$  are  
328 predominantly blood-flow dependent (Figure 5 D and E), whereas the other modalities are  
329 both influenced by blood flow and blood content differences (Figures 4 C and D and 5 C). All  
330 models were significant, with  $r^2$  from 0.58 to 0.59 for lung gas exchange models and 0.69 to  
331 0.95 for models of gas exchange at the ECMO (Equation data in e-table 4 in the online  
332 supplement). The calculated  $\dot{V}/\dot{Q}$  ratio used for the  $\dot{V}CO_2$  normalization shows a median

333 value of 1.26 for baseline conditions, 0.58 for shunt conditions, and 1.43 for deadspace  
334 conditions (e-Figure 4 in the online supplement).

335

## DISCUSSION

336

337 In this study, we could show that a modified Fick principle estimates native cardiac output  
338 with high accuracy but considerable lack in precision in the setting of VA-ECMO. Shunt  
339 creation led to systematic underestimation of true blood flow, whereas dead space creation  
340 did not change the accuracy of the method. Accuracy and precision of the cardiac output  
341 estimates depend on the measurement technique (blood vs. gas phase) and the gas chosen  
342 (oxygen vs. carbon dioxide) and will be further elaborated below.

343

344 As a major limitation of the experimental setup, we used healthy animals in our model. This  
345 allowed standardized investigations and controlled induction of shunt and dead space, but  
346 may not resemble clinical situations of complex disturbances in gas exchange by either  
347 shock or lung failure. Further limitations are the use of a side-stream capnograph for oxygen  
348 measurements and the lack of appropriate blood content models for pigs, particularly carbon  
349 dioxide. We could also not verify our estimates of the  $\dot{V}/\dot{Q}$  ratio at the lung, which we needed  
350 for the normalization procedure, with an independent technique like MIGET or impedance  
tomography.

351

352 Cardiac output measurements are notoriously imprecise. Limits of agreement of +/- 30% are  
353 considered the limit for the acceptance of a new measurement method for clinical use (10),  
354 but even larger bands up to 45% are discussed. For  $\dot{V}O_{2\text{ Blood}}$  (i.e. a classic Fick approach),  
355 we reached clinically acceptable accuracy and precision, with acceptable trending ability  
356 (23). For other modalities of gas exchange, particularly measurements in the gas phase, the  
357 results are limited for clinical application by their lack of precision. Although gaseous  
358 measurements are noninvasive and could be easily implemented in a clinical setting, our  
359 results show their inherent limitations. The results are highly dependent on the measurement  
360 technique for exhaust and exhaled gases. The normalization procedure, although dependent  
361 on an estimation of  $\dot{V}/\dot{Q}$  at the lung, which we could not verify independently, improves the  
accuracy and precision substantially.

362

363 We identify three substantial contributors to the imprecision in blood flow calculations based  
364 on our modified Fick principle: First, the measurement techniques (capnography and derived  
365 oxygen consumption) have inherent inaccuracies. The capnostat 5 device has a  
366 measurement accuracy of  $\pm 2$  mmHg below 41 mmHg and  $\pm 5\%$  of the reading in the range  
367 of 41 to 71 mmHg. The manufacturer of the E-COVX side-stream module reports an  
368 accuracy of  $\pm (0.2 \text{ vol } \% + 2\% \text{ of the reading})$  for carbon dioxide, and  $\pm (1 \text{ vol } \% + 2\% \text{ of the}$   
369  $\text{reading})$  for oxygen. In addition, synchronization problems of expiratory tidal flow and side-  
370 stream measurements of oxygen may have occurred. Both may be overcome in the future by  
more precise measurement probes and the use of volumetric capno- or oxygraphs.

371 Furthermore, gas content calculations of carbon dioxide are insufficient and only human  
372 models exist (22). The error in blood content resulting from the transfer between blood and  
373 gas measurements is described in e-Figure 2. Linear mixed-effect models (Figure 4 and 5)  
374 reveal a significant relationship between the relevant factors determining  $\dot{V}O_2/\dot{V}CO_2$ .  
375 Gaseous measurements at the ECMO outlet are more accurate, because there is constant  
376 flow and the applied Haldane transformation allows precise calculation of gas flow at the  
377 ECMO outlet with oxygen concentrations below 0.6.

378 The ability of an ECMO system to remove carbon dioxide at high V/Q ratios leads to the  
379 clinical commonplace that carbon dioxide elimination is completely independent of blood  
380 flow, which is not the case.  $\dot{V}/\dot{Q}$  ratios that are unequal to 1 will influence the amount of  
381 carbon dioxide removed from the blood and thus interfere with the accuracy of the presented  
382 method. Similarly, low  $\dot{V}/\dot{Q}$  ratios at the lung lead to low oxygen saturations (Figure 4 B). The  
383 normalization procedure can empirically correct for this but is dependent on the accuracy of  
384 the  $\dot{V}/\dot{Q}$  estimation at the lung, which we could not verify independently. Of note is the  
385 corrected bias presented in Figure 3D for the shunt condition, which shows the effect of  
386 normalization. Although the bias for shunt in general is negative because of an expected  
387 underestimation resulting from blood flow not participating in gas exchange, the  
388 normalization procedure can correct not only for high  $\dot{V}/\dot{Q}$  ( $> 1$ ) but also for this low  $\dot{V}/\dot{Q}$   
389 distribution. The effect of the normalization procedure is visualized through the linear mixed-  
390 effects model in Figure 5 E, where  $\dot{V}CO_2$  becomes dependent only on blood flow and is  
391 independent of differences in gas content, which allows for better precision in blood flow  
392 calculations.

393 The proposed mass balance equations (Eq. 3A and B) are true only if both circuits are  
394 participating in the gas exchange of the entire body, resulting in equal inflow conditions, and  
395 if the amount of gas exchanged is the same, resulting in equal outflow conditions. As shown  
396 in Figures 4 and 5, this is the case for neither oxygen nor carbon dioxide in our experimental  
397 setup. While clinicians are familiar with the differences in the outflow content and recognize it  
398 at the bedside as differential hypoxia or the Harlequin phenomenon (8, 12), the content  
399 differences on the venous side are less known. These may have considerable impact on  
400 cannulation choice and effectiveness (16) and may even lead to wrong clinical conclusions,  
401 when inflow saturation are considered as a surrogate for true mixed venous blood (i. e. blood  
402 from the pulmonary artery), as it is recommended practice (31). It may be of further note that  
403 the usual calculations for gas exchange calculations on ECMO (32, 38) usually do not  
404 consider differences in inflow ("mixed") venous saturations or carbon dioxide concentrations.

405 Third, we have previously used differences in  $\dot{V}CO_2$  between ECMO flow changes to  
406 calculate changes in blood flow (3). In this current study, we applied the same technique to

407 continuous direct measurements of gas exchange rather than applying the technique for the  
408 differences between weaning steps. However, our results show that a steady state is  
409 essentially not reached with changing total  $\dot{V}CO_2$  (online supplement). This results in  
410 changing conditions (e.g. total  $\dot{V}CO_2$  removal), which directly influences our blood flow  
411 calculations. Giosa et al. have demonstrated that carbon dioxide stores are substantial and a  
412 steady state of carbon dioxide exchange may be achieved only over hours or even days (13).  
413 We chose three-minute measurement intervals empirically. This approximates the time  
414 resolution of a fast-responding cardiac output thermodilution system (25), but also may  
415 reduce the error introduced by a breath-by-breath system (24). Whether this measurement  
416 period could be further optimized needs to be studied further. Mainly these technical  
417 limitations of our approach may be overcome in future practice. Measurements of gas  
418 exchange at the ECMO using the Haldane transformation are accurate. Precise real-time  
419 measurements of  $\dot{V}O_2$  through new technologies such as molecular inflow gas spectroscopy  
420 may substantially improve our approach and enable precision demonstrated by  
421 measurements of  $\dot{V}O_{2\text{ Blood}}$  (9). A steady state for  $\dot{V}O_2$  is much more easily reached, as body  
422 stores are insubstantial, and is indirectly shown by our blood content calculations.

423 This data set is to our knowledge the largest documentation of gas exchange and its  
424 distribution between native and artificial lung in an experimental model of V-A ECMO. Our  
425 data show that there is a clear distribution of oxygen uptake and carbon dioxide removal  
426 between the two circuits with a respective transfer of gas exchange load through flow  
427 changes. The presented method may aid in evaluating the function of the native  
428 cardiopulmonary unit not only through monitoring of the gas exchange distribution but also  
429 through direct assessment of sufficient gas exchange transfer. The venous inlet of the ECMO  
430 circuit and the blood that flows through the pulmonary artery show substantial differences in  
431 oxygen content and carbon dioxide tension. The amount of oxygen uptake through the  
432 ECMO circuit is limited by the venous saturation, a fact that is also important for veno-venous  
433 (V-V) ECMO configurations (39). The differences between pulmonary artery and venous  
434 ECMO saturations also imply that central venous saturations are an insufficient surrogate for  
435 mixed venous saturations (Figure 7A), a finding that has been reproduced by other studies  
436 (21).

437 In conclusion, our modified Fick principle produces clinically accurate and precise  
438 measurements of native cardiac output on V-A ECMO, when based on blood oxygen  
439 content. When other gases are used, steady state behavior and technical measurement  
440 inaccuracies may significantly contribute to imprecision. Normalizing toward a  $\dot{V}/\dot{Q}$  ratio of 1  
441 improves accuracy and precision. The inflow gas content between membrane lung and  
442 natural lung are significantly different and should be taken into account for mass balance  
443 equations on V-A and presumably V-V ECMO.



444 In conclusion, our modified Fick principle for the estimation of cardiac output on VA-ECMO  
445 may offer a continuous measurement possibility for monitoring these patients in the future,  
446 when precision may be improved by further developments in expired gas measurement  
447 techniques. For current practice and management, and also for the development of  
448 mathematical models of ECMO gas exchange, it must be recognized that differential hypoxia  
449 is not a limited phenomenon on the arterial side, but also exists between the ECMO inflow  
450 and the pulmonary artery.

## 451 ACKNOWLEDGMENTS

452 We would like to thank Peter Robbins from the Department of Physiology, University of  
453 Oxford for his help and insightful discussions of the method and manuscript.

## 454 REFERENCES

- 455 1. **Abrams D, Maclaren G, Lorusso R, Price S, Yannopoulos D, Vercaemst L,**  
456 **Bělohávek J, Taccone FS, Aissaoui N, Shekar K, Garan AR, Uriel N, Tonna JE, Jung**  
457 **JS, Takeda K, Chen Y-S, Slutsky AS, Combes A, and Brodie D.** Extracorporeal  
458 cardiopulmonary resuscitation in adults: evidence and implications. *Intensive care medicine*,  
459 2021.
- 460 2. **Bachmann KF and Berger D.** Impaired membrane lung CO<sub>2</sub> elimination: is it dead  
461 space, V/Q ratio or acidosis? *Perfusion* 35: 875-877, 2020.
- 462 3. **Bachmann KF, Haenggi M, Jakob SM, Takala J, Gattinoni L, and Berger D.** Gas  
463 exchange calculation may estimate changes in pulmonary blood flow during veno-arterial  
464 extracorporeal membrane oxygenation in a porcine model. *American journal of physiology*  
465 *Lung cellular and molecular physiology* 318: L1211-L1221, 2020.
- 466 4. **Bachmann KF, Vasireddy R, Heinisch PP, Jenni H, Vogt A, and Berger D.**  
467 Estimating cardiac output based on gas exchange during veno-arterial extracorporeal  
468 membrane oxygenation in a simulation study using paediatric oxygenators. *Sci Rep* 11:  
469 11528, 2021.
- 470 5. **Bachmann KF, Zwicker L, Nettelbeck K, Casoni D, Heinisch PP, Jenni H,**  
471 **Haenggi M, and Berger D.** Assessment of Right Heart Function during Extracorporeal  
472 Therapy by Modified Thermodilution in a Porcine Model. *Anesthesiology* 133: 879-891, 2020.
- 473 6. **Bland JM and Altman DG.** Measuring agreement in method comparison studies.  
474 *Statistical Methods in Medical Research* 8: 135-160, 1999.
- 475 7. **Bland JM and Altman DG.** Statistical methods for assessing agreement between two  
476 methods of clinical measurement. *Lancet* 1: 307-310, 1986.

- 477 8. **Choi JH, Kim SW, Kim YU, Kim S-Y, Kim K-S, Joo S-J, and Lee JS.** Application of  
478 veno-arterial-venous extracorporeal membrane oxygenation in differential hypoxia.  
479 *Multidisciplinary Respiratory Medicine* 9: 55, 2014.
- 480 9. **Ciaffoni L, O'Neill DP, Couper JH, Ritchie GA, Hancock G, and Robbins PA.** In-  
481 airway molecular flow sensing: A new technology for continuous, noninvasive monitoring of  
482 oxygen consumption in critical care. *Sci Adv* 2: e1600560, 2016.
- 483 10. **Critchley LA, Lee A, and Ho AMH.** A critical review of the ability of continuous  
484 cardiac output monitors to measure trends in cardiac output. *Anesthesia and analgesia* 111:  
485 1180-1192, 2010.
- 486 11. **Dash RK and Bassingthwaighte JB.** Erratum to: Blood HbO<sub>2</sub> and HbCO<sub>2</sub>  
487 dissociation curves at varied O<sub>2</sub>, CO<sub>2</sub>, pH, 2,3-DPG and temperature levels. *Annals of*  
488 *biomedical engineering* 38: 1683-1701, 2010.
- 489 12. **Falk L, Sallisalmi M, Lindholm JA, Lindfors M, Frenckner B, Broomé M, and**  
490 **Broman LM.** Differential hypoxemia during venoarterial extracorporeal membrane  
491 oxygenation. *Perfusion* 34: 22-29, 2019.
- 492 13. **Giosa L, Busana M, Bonifazi M, Romitti F, Vassalli F, Pasticci I, Macri MM,**  
493 **D'Albo R, Collino F, Gatta A, Palumbo MM, Herrmann P, Moerer O, Iapichino G,**  
494 **Meissner K, Quintel M, and Gattinoni L.** Mobilizing Carbon Dioxide Stores. An  
495 Experimental Study. *American journal of respiratory and critical care medicine* 203: 318-327,  
496 2021.
- 497 14. **Hannon JP, Bossone CA, and Wade CE.** Normal physiological values for conscious  
498 pigs used in biomedical research. *Laboratory animal science* 40: 293-298, 1990.
- 499 15. **Herner A, Lahmer T, Mayr U, Rasch S, Schneider J, Schmid RM, and Huber W.**  
500 Transpulmonary thermodilution before and during veno-venous extra-corporeal membrane  
501 oxygenation ECMO: an observational study on a potential loss of indicator into the extra-  
502 corporeal circuit. *Journal of clinical monitoring and computing* 34: 923-936, 2020.
- 503 16. **Hou X, Yang X, Du Z, Xing J, Li H, Jiang C, Wang J, Xing Z, Li S, Li X, Yang F,**  
504 **Wang H, and Zeng H.** Superior vena cava drainage improves upper body oxygenation  
505 during veno-arterial extracorporeal membrane oxygenation in sheep. *Critical Care* 19: 68,  
506 2015.
- 507 17. **Keener JS, J.** Ventilation and Perfusion. In: *Mathematical Physiology: Systems*  
508 *Physiology* (Second Edition ed.), edited by Antman SM, J. Sirovich L. New York: Springer,  
509 2009, p. 694-701.
- 510 18. **Khorsandi M, Dougherty S, Bouamra O, Pai V, Curry P, Tsui S, Clark S, Westaby**  
511 **S, Al-Attar N, and Zamvar V.** Extra-corporeal membrane oxygenation for refractory  
512 cardiogenic shock after adult cardiac surgery: a systematic review and meta-analysis.  
513 *Journal of Cardiothoracic Surgery* 12, 2017.

- 514 19. **Kowalewski M, Zieliński K, Brodie D, MacLaren G, Whitman G, Raffa GM,**  
515 **Boeken U, Shekar K, Chen YS, Bermudez C, D'Alessandro D, Hou X, Haft J, Belohlavek**  
516 **J, Dziembowska I, Suwalski P, Alexander P, Barbaro RP, Gaudino M, Di Mauro M,**  
517 **Maessen J, and Lorusso R.** Venoarterial Extracorporeal Membrane Oxygenation for  
518 Postcardiotomy Shock-Analysis of the Extracorporeal Life Support Organization Registry.  
519 *Crit Care Med* 49: 1107-1117, 2021.
- 520 20. **Kowalewski M, Zieliński K, Maria Raffa G, Meani P, Lo Coco V, Jiritano F, Fina**  
521 **D, Matteucci M, Chiarini G, Willers A, Simons J, Suwalski P, Gaudino M, Di Mauro M,**  
522 **Maessen J, and Lorusso R.** Mortality Predictors in Elderly Patients With Cardiogenic Shock  
523 on Venoarterial Extracorporeal Life Support. Analysis From the Extracorporeal Life Support  
524 Organization Registry. *Crit Care Med* 49: 7-18, 2021.
- 525 21. **Lanning KM, Erkinaro TM, Ohtonen PP, Vakkala MA, Liisanantti JH, Ylikauma**  
526 **LA, and Kaakinen TI.** Accuracy, Precision, and Trending Ability of Perioperative Central  
527 Venous Oxygen Saturation Compared to Mixed Venous Oxygen Saturation in Unselected  
528 Cardiac Surgical Patients. *Journal of cardiothoracic and vascular anesthesia*, 2021.
- 529 22. **O'Neill DP and Robbins PA.** A mechanistic physicochemical model of carbon  
530 dioxide transport in blood. *J Appl Physiol (1985)* 122: 283-295, 2017.
- 531 23. **Odor PM, Bampoe S, and Cecconi M.** Cardiac Output Monitoring: Validation  
532 Studies-how Results Should be Presented. *Current anesthesiology reports* 7: 410-415, 2017.
- 533 24. **Peyton PJ, Venkatesan Y, Hood SG, Junor P, and May C.** Noninvasive, automated  
534 and continuous cardiac output monitoring by pulmonary capnodynamics: breath-by-breath  
535 comparison with ultrasonic flow probe. *Anesthesiology* 105: 72-80, 2006.
- 536 25. **Reuter DA, Huang C, Edrich T, Shernan SK, and Eltzschig HK.** Cardiac output  
537 monitoring using indicator-dilution techniques: basics, limits, and perspectives. *Anesthesia*  
538 *and analgesia* 110: 799-811, 2010.
- 539 26. **Rik.** BlandAltmanPlot 2019.
- 540 27. **Sackner MA.** Measurement of Cardiac Output by Alveolar Gas Exchange. In:  
541 *Comprehensive Physiology*, p. 233-255.
- 542 28. **Serianni R, Barash J, Bentley T, Sharma P, Fontana JL, Via D, Duhm J, Bunger**  
543 **R, and Mongan PD.** Porcine-specific hemoglobin saturation measurements. *Journal of*  
544 *Applied Physiology* 94: 561-566, 2003.
- 545 29. **Shekar K, Donker DW, and Brodie D.** Venoarterial Extracorporeal Membrane  
546 Oxygenation: If You Cannot Measure It, You Cannot Improve It. *Anesthesiology* 133: 708-  
547 710, 2020.
- 548 30. **Smith M, Vukomanovic A, Brodie D, Thiagarajan R, Rycus P, and Buscher H.**  
549 Duration of veno-arterial extracorporeal life support (VA ECMO) and outcome: an analysis of  
550 the Extracorporeal Life Support Organization (ELSO) registry. *Critical care* 21: 45, 2017.

- 551 31. **Su Y, Liu K, Zheng J-L, Li X, Zhu D-M, Zhang Y, Zhang Y-J, Wang C-S, SHI T-T,**  
552 **Luo Z, and Tu G-W.** Hemodynamic monitoring in patients with venoarterial extracorporeal  
553 membrane oxygenation. *Annals of translational medicine* 8: 792, 2020.
- 554 32. **Sun L, Kaesler A, Fernando P, Thompson AJ, Toomasian JM, and Bartlett RH.**  
555 CO<sub>2</sub> clearance by membrane lungs. *Perfusion* 33: 249-253, 2018.
- 556 33. **Takala J.** Gas Exchange and Indirect Calorimetry.
- 557 34. **Takala J and Meriläinen P.** *Handbook of Gas Exchange and Indirect Calorimetry.*  
558 Datex, 1991.
- 559 35. **Wagner PD.** The multiple inert gas elimination technique (MIGET). *Intensive care*  
560 *medicine* 34: 994-1001, 2008.
- 561 36. **Wilmore JH and Costill DL.** Adequacy of the Haldane transformation in the  
562 computation of exercise V O<sub>2</sub> in man. *Journal of applied physiology* 35: 85-89, 1973.
- 563 37. [www.physiome.org](http://www.physiome.org). Blood HbO<sub>2</sub> and HbCO<sub>2</sub> Dissociation Curves at Varied O<sub>2</sub>,  
564 CO<sub>2</sub>, pH, 2,3-DPG and Temperature Levels. Based directly on Dash et al. 2010 errata  
565 reprint., 2020, p. Model number: 0149.
- 566 38. **Zanella A, Salerno D, Scaravilli V, Giani M, Castagna L, Magni F, Carlesso E,**  
567 **Cadringher P, Bombino M, Grasselli G, Patroniti N, and Pesenti A.** A mathematical  
568 model of oxygenation during venovenous extracorporeal membrane oxygenation support.  
569 *Journal of critical care* 36: 178-186, 2016.
- 570 39. **Zante B, Berger DC, Schefold JC, and Bachmann KF.** Dissociation of Arterial  
571 Oxygen Saturation and Oxygen Delivery in VV-ECMO: The Trend Is Your Friend. *J*  
572 *Cardiothorac Vasc Anesth* 35: 962-963, 2021.

573 This manuscript contains an online supplement available at

574 <https://doi.org/10.6084/m9.figshare.19070132> (individual animal data)

575 <https://doi.org/10.6084/m9.figshare.20489439> (additional results)

576

577

578 **FIGURES**

579 **FIGURE LEGENDS**

580

581 **Figure 1. A:** Experimental setup. ABP: Arterial/systemic blood pressure. AO: aorta. ECMO:  
582 Extracorporeal membrane oxygenation. LA: Left atrium. LAP: Left atrial pressure. PA:  
583 Pulmonary artery. PAP: Pulmonary artery pressure. RA: Right atrium. RAP: Right atrial  
584 pressure. **B:** Experimental conditions. BF: Blood flow. BW: Body weight. BGA: Blood gas  
585 analysis.

586 **Figure 2.** Cardiac output calculations based on oxygen content

587 **A:** Bland–Altman plot for calculated cardiac output using blood measurements of  $\dot{V}O_{2\text{ Blood}}$ .

588 Percentage errors: Baseline 36.4%. Shunt 51.0%. Dead space 35.1%. Regression  
589 equations are given in the online supplement

590 **B:** Trending abilities for  $\dot{V}O_{2\text{ Blood}}$ . Regression equations are given in the online supplement.

591 **C:** Bland–Altman plot for calculated cardiac output using blood measurements of  $\dot{V}O_{2\text{ Gas}}$

592 Percentage errors: Baseline 91.4%. Shunt 71.3%. Dead space 98.8%. Regression  
593 equations are given in the online supplement

594 **D:** Trending abilities for  $\dot{V}O_{2\text{ Gas}}$ . Regression equations are given in the online supplement.

595

596 **Figure 3.** Cardiac output calculations based on carbon dioxide content

597 **A:** Bland–Altman plot for calculated cardiac output using measurements of  $\dot{V}CO_{2\text{ Gas}}$ .

598 Percentage errors: Baseline 72.6%. Shunt 70.5%. Dead space 79.2%.

599 **B:** Trending abilities for  $\dot{V}CO_{2\text{ Gas}}$ . Regression equations are given in the online supplement.

600 **C:** Bland–Altman plot for calculated cardiac output using measurements of  $\dot{V}CO_{2\text{ Gas Norm}}$

601 Percentage errors: Baseline 70.5%. Shunt 58.2%. Dead space 83.2%.

602 **D:** Trending abilities for  $\dot{V}CO_{2\text{ Gas Norm}}$ . Regression equations are given in the online  
603 supplement.

604 **Figure 4.** *Influencing factors on the cardiac output calculations based on oxygen content*

605 Inflow (venous ECMO drainage and pulmonary artery) and outflow (arterial ECMO limb and  
606 left atrium) blood gas content for venous oxygen saturation ( $sO_2$ ; bias -0.9% [-1.2 to -0.5%],

607 limits of agreement -11.2 to 11.4%; **A**) and arterial  $sO_2$  (bias -2.5% [-3.0 to -2.0%], limits of  
608 agreement -18.6 to 13.6%; **B**).

609

610 Linear mixed-effect models assessing the relationship between difference in blood gas  
611 content, blood flow, and gaseous measurements of gas exchange for **(C)**  $\dot{V}O_{2\text{ Lung}}$ , **(C)**  $\dot{V}O_{2\text{ ECMO}}$ . The planes represent the model estimates. Model parameters are given in the online  
612 supplement. LA: Left atrium. PA: Pulmonary artery

613

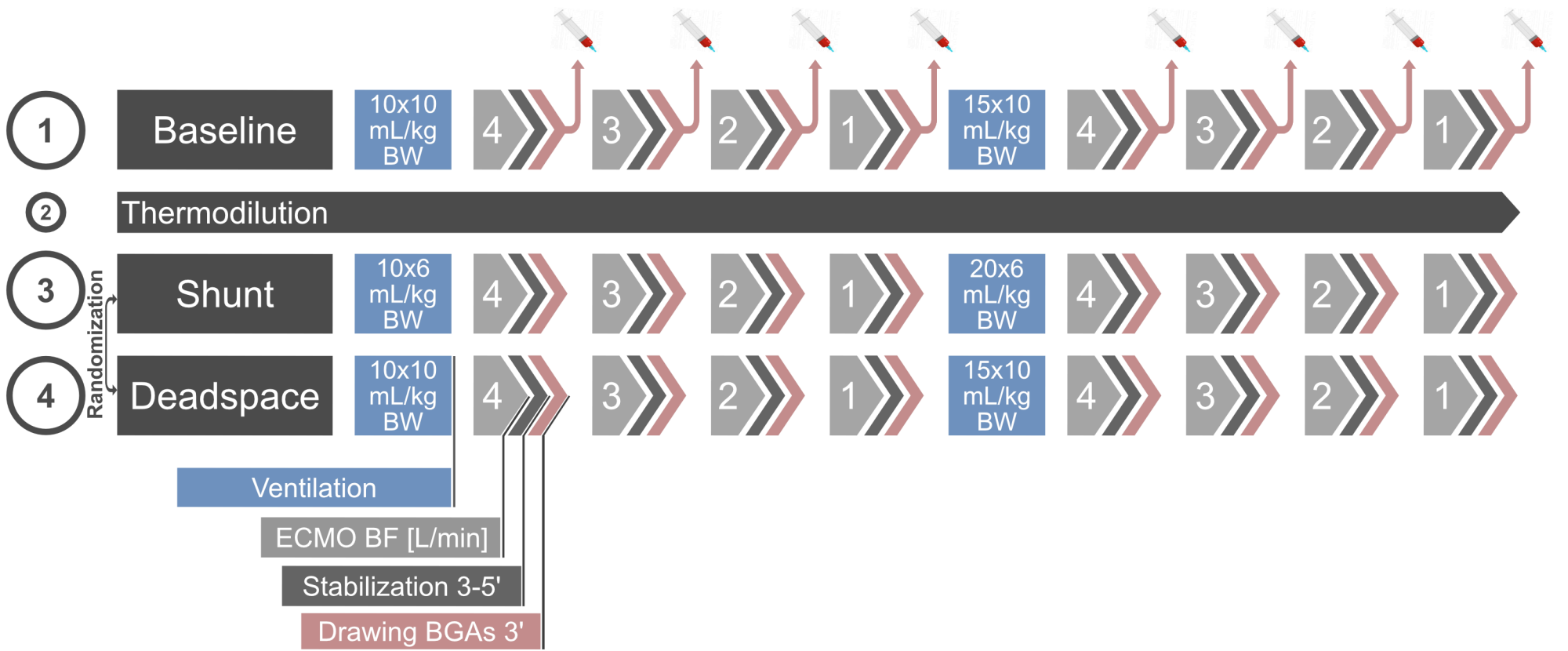
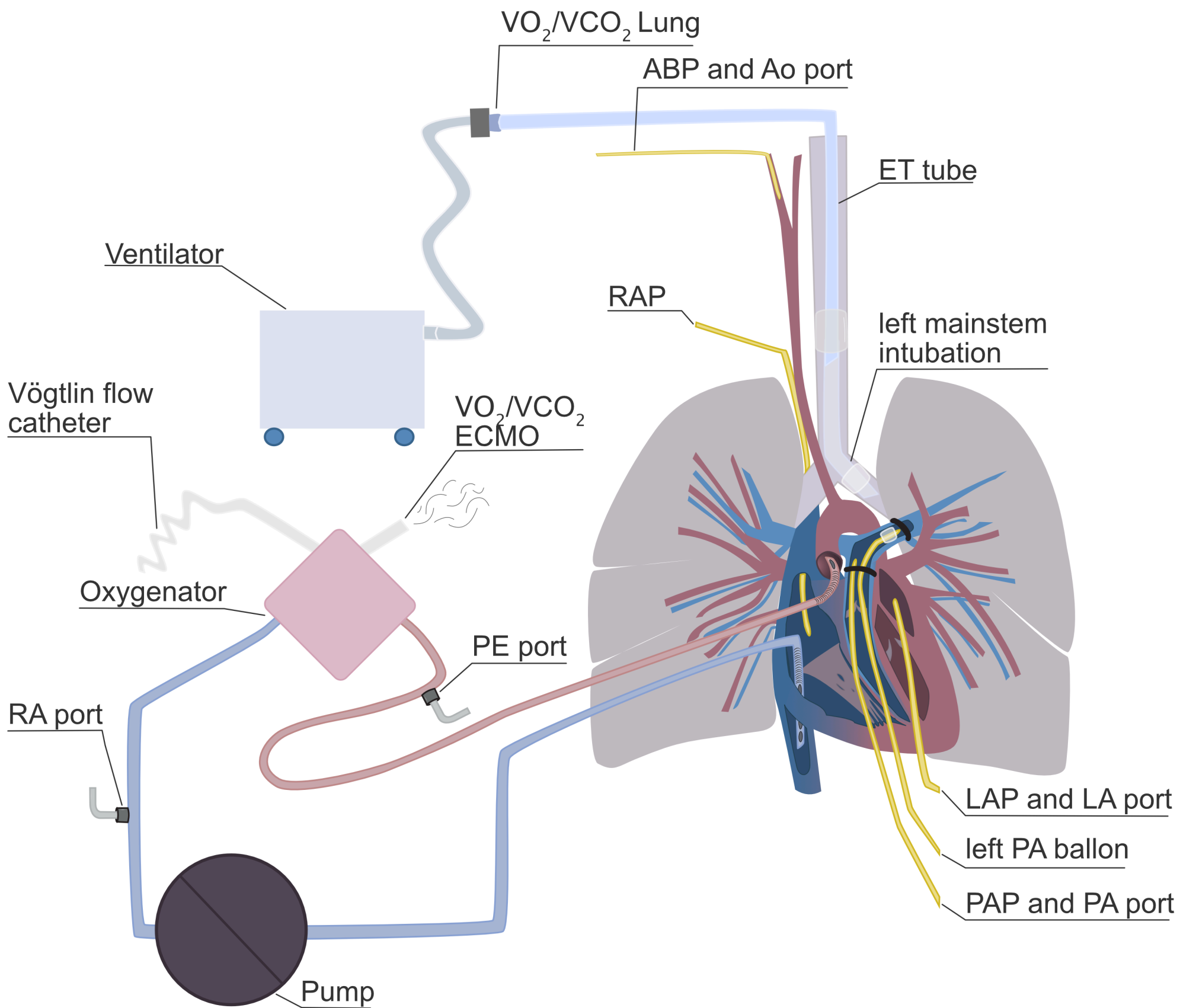
614  
615 **Figure 5.** *Influencing factors on the cardiac output calculations based on carbon dioxide*  
616 *content*

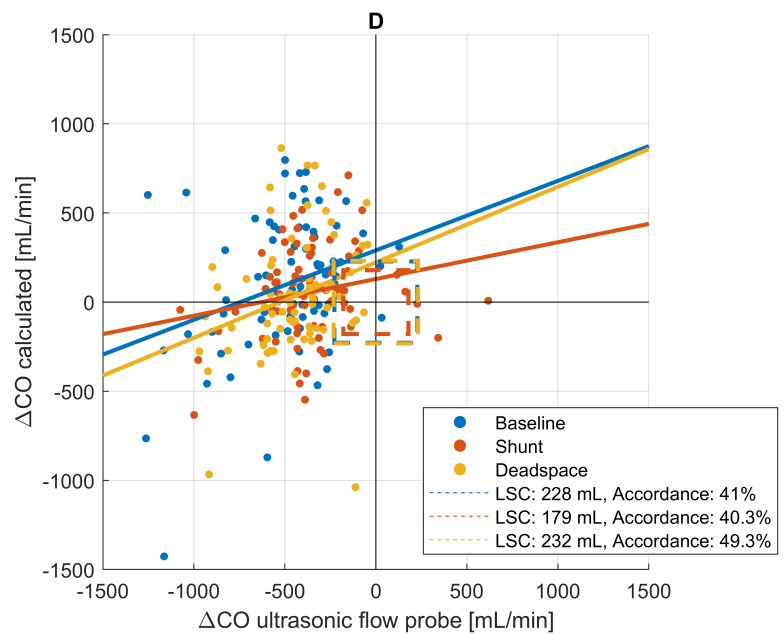
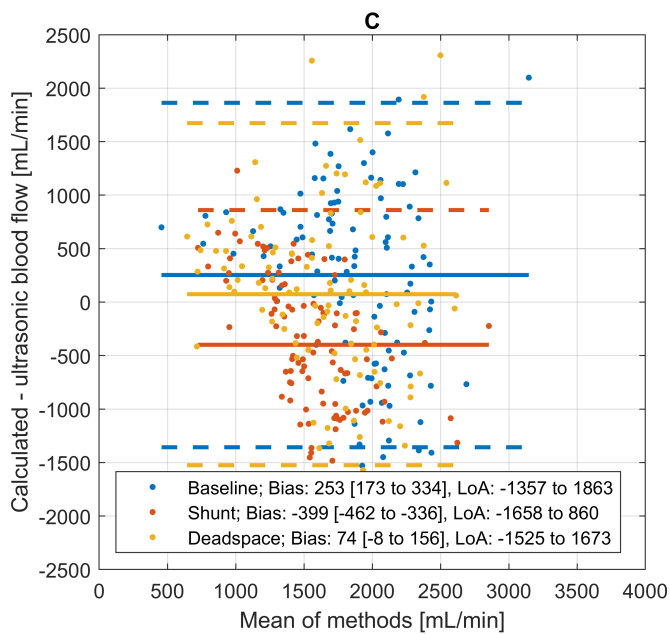
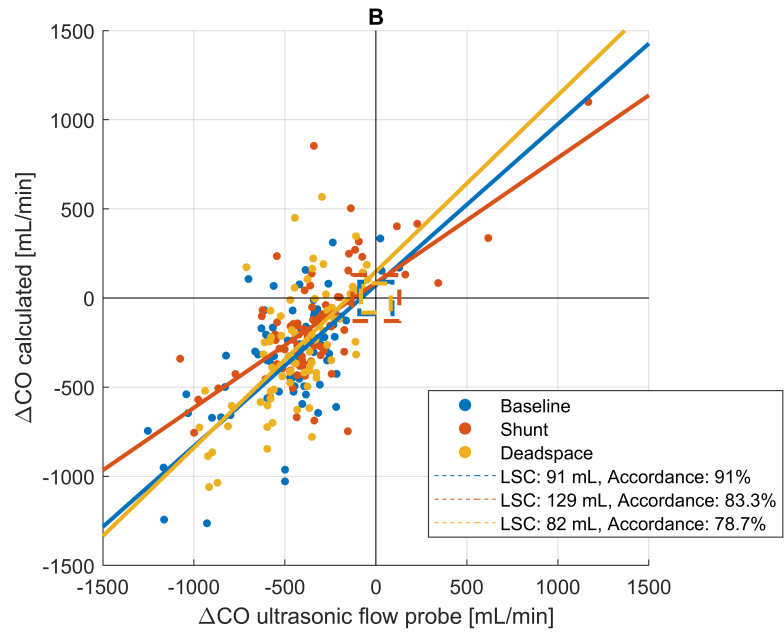
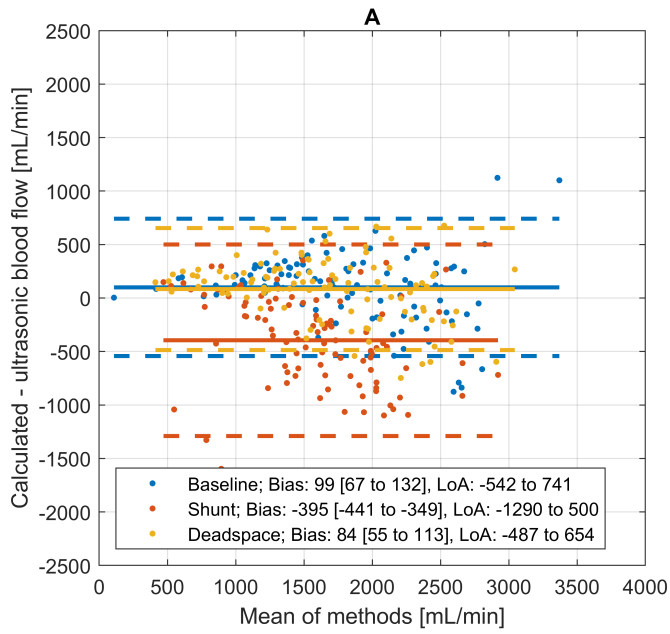
617 Inflow (venous ECMO drainage and pulmonary artery) and outflow (arterial ECMO limb and  
618 left atrium) blood gas content for venous partial pressure of carbon dioxide ( $pCO_2$ ; bias -0.86  
619 mmHg, limits of agreement -4.72 to 3.00 mmHg; **A**) and arterial  $pCO_2$  (bias 3.66 mmHg [3.28  
620 to 4.05 mmHg], limits of agreement -9.59 to 16.92 mmHg; **B**).

621 Linear mixed-effect models assessing the relationship between difference in blood gas  
622 content, blood flow, and gaseous measurements for  $\dot{V}CO_{2\text{ Lung}}$ , **(C)**  $\dot{V}CO_{2\text{ ECMO}}$ , **(D)** and  $VCO_{2\text{ Norm Lung}}$  **(E)**. The planes represent the model estimates. Model parameters are given in the  
623 online supplement. ECMO: Extracorporeal membrane oxygenation. Norm: Normalized. LA:  
624 Left atrium. PA: Pulmonary artery

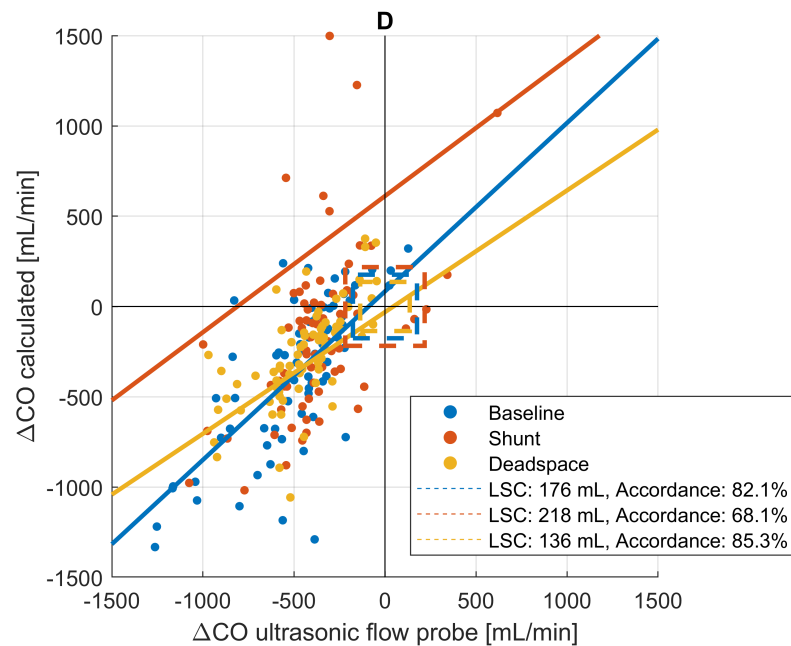
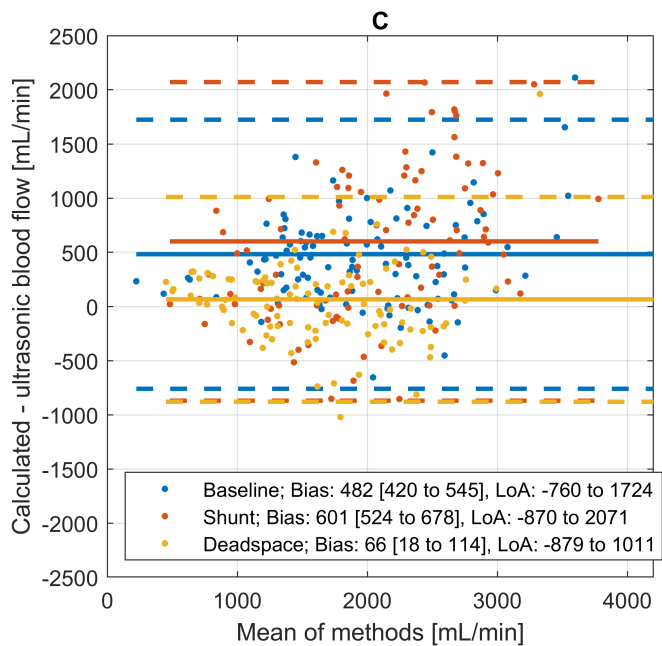
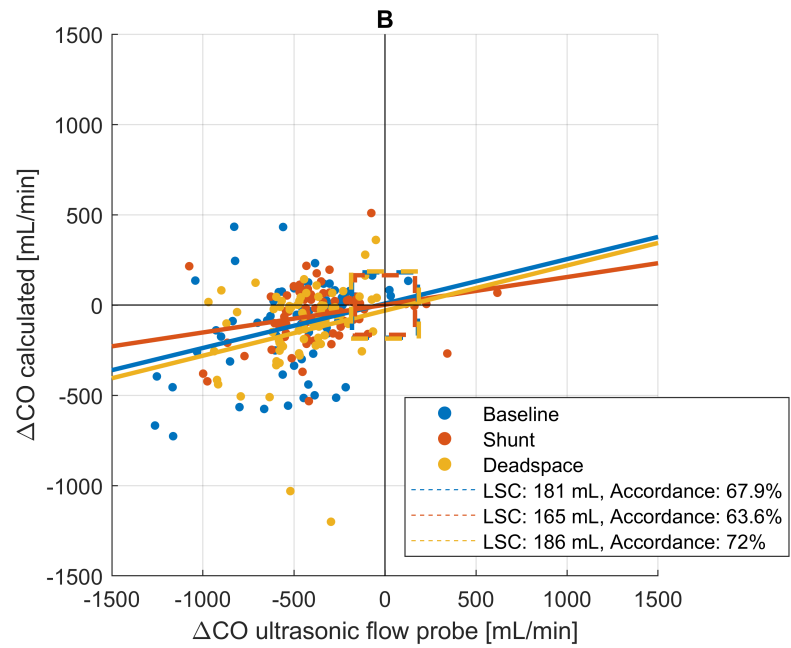
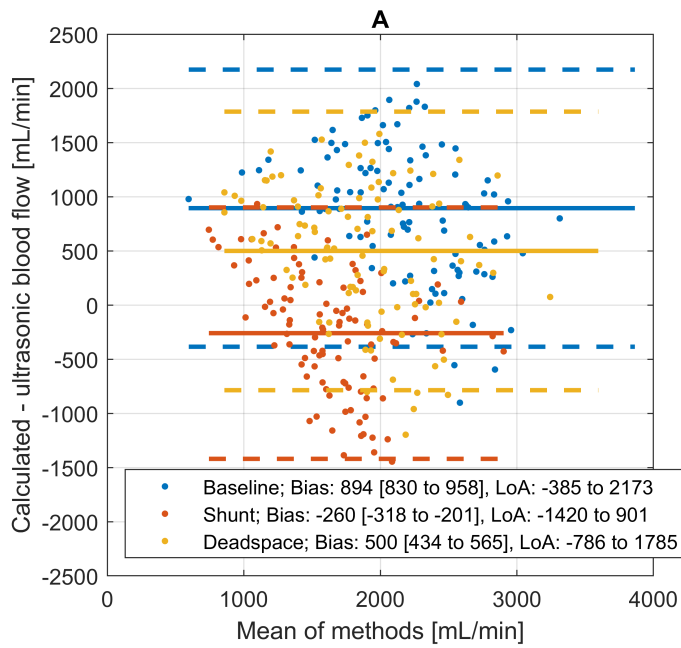
625

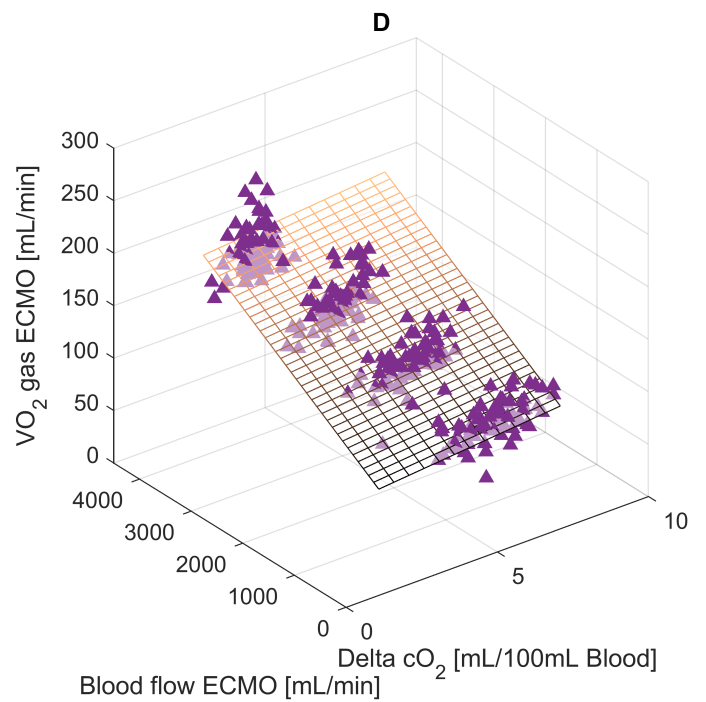
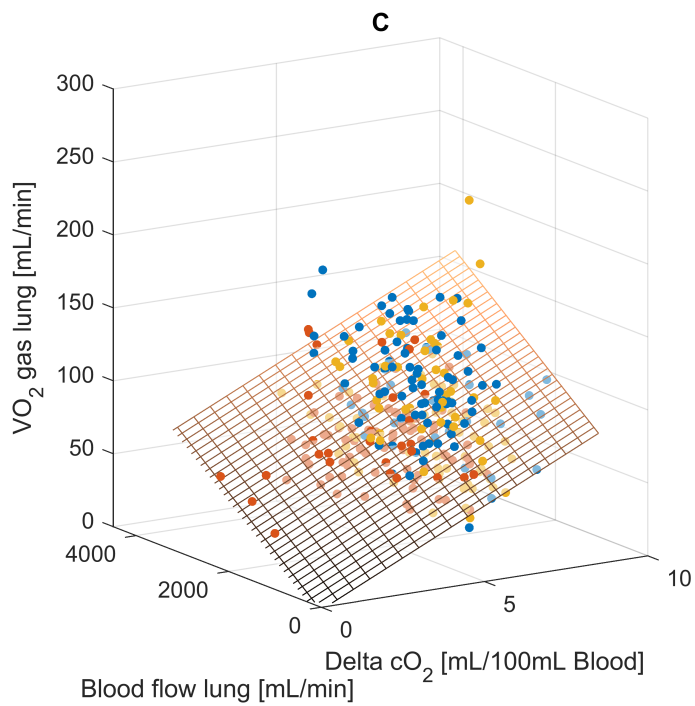
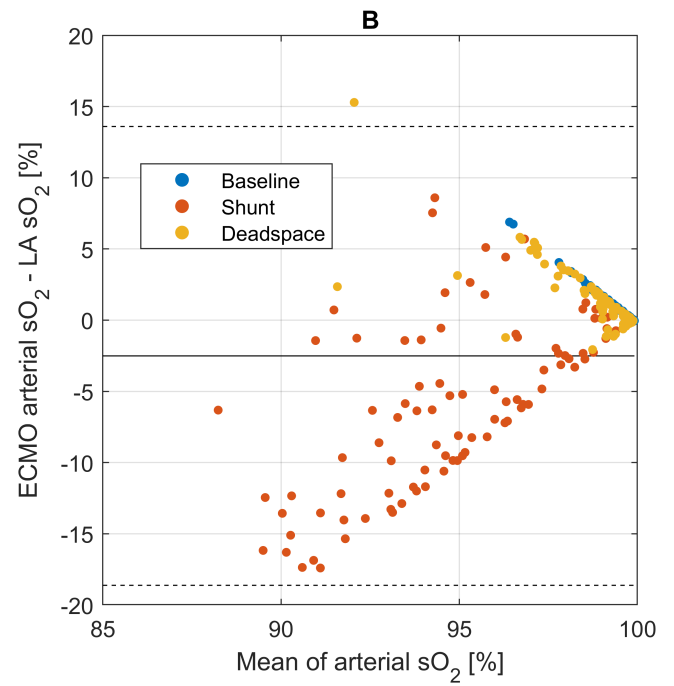
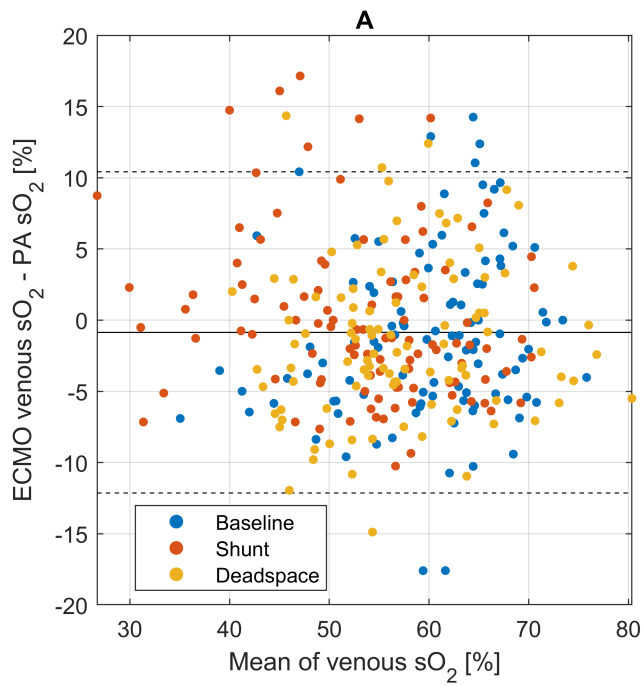
626

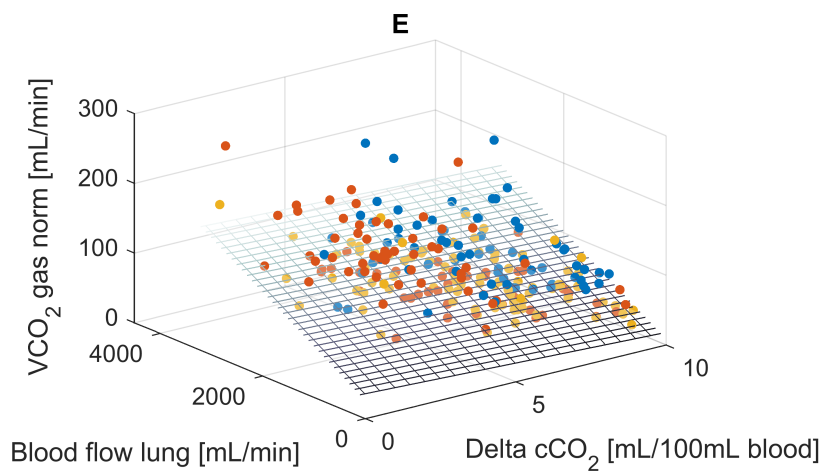
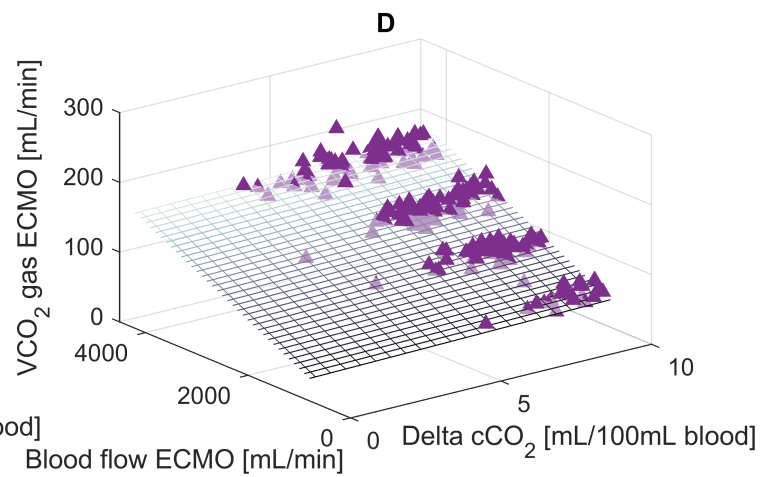
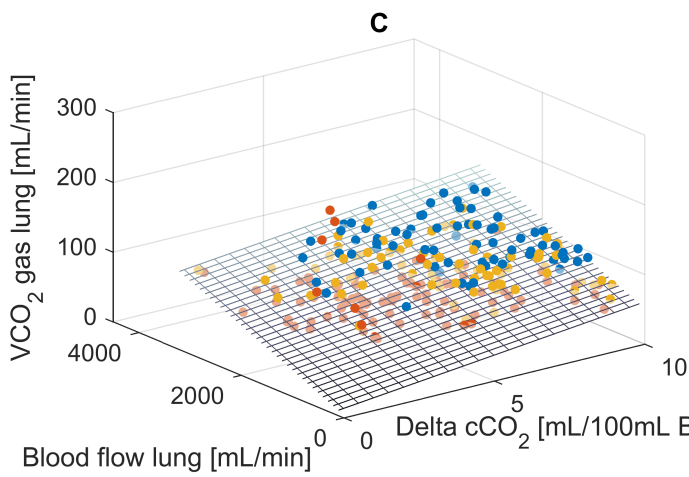
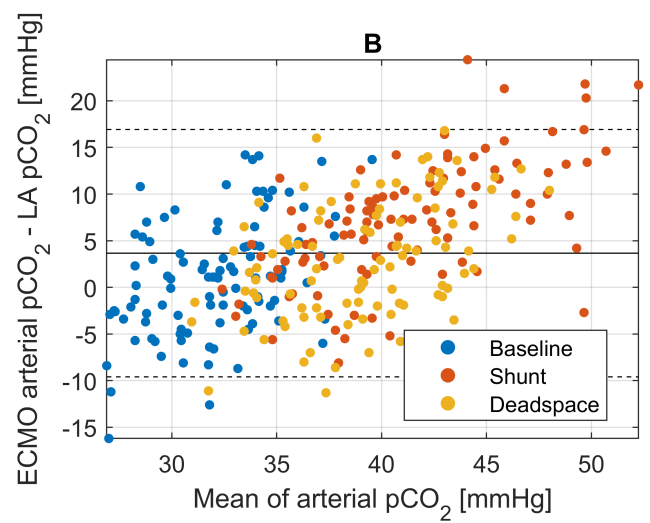
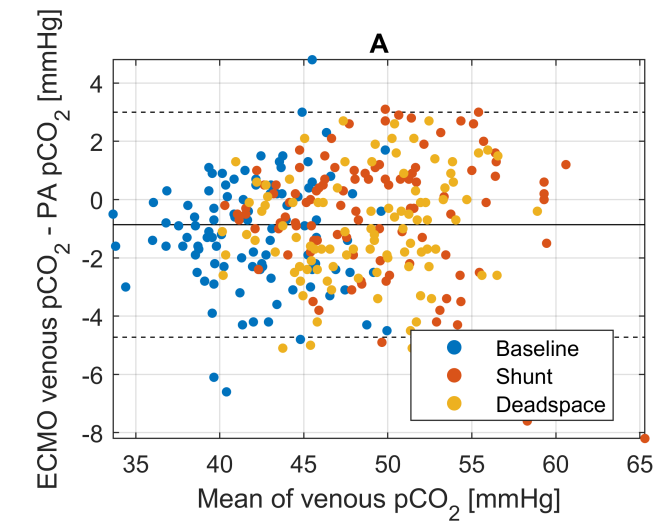
**A****B**





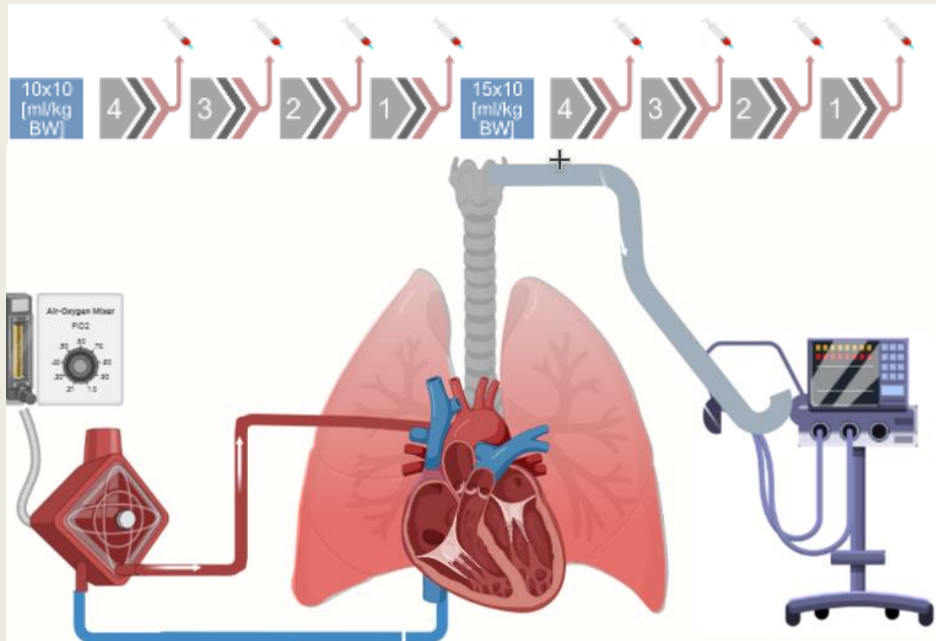






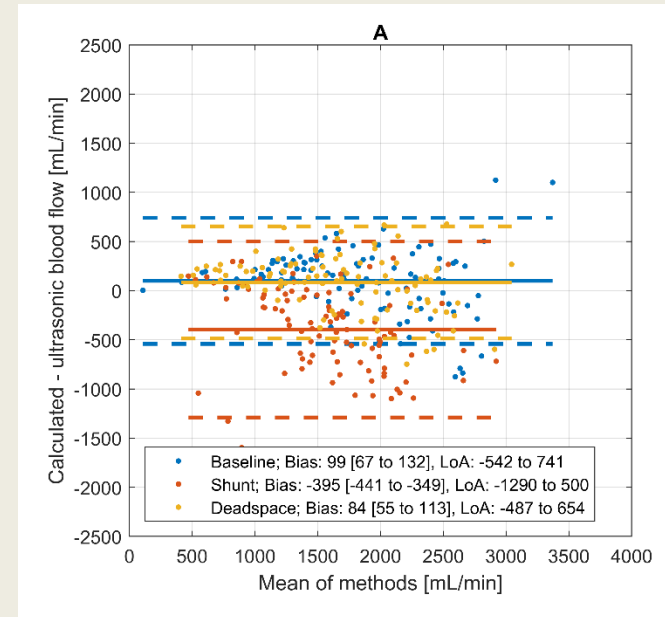
# A Modified Fick Principle in veno-arterial Extracorporeal Membrane Oxygenation

## METHODS



13 pigs were weaned from a veno-arterial membrane lung with simultaneous assessment of gas exchange ( $\text{VO}_2$  &  $\text{VCO}_2$ ) at the native and the membrane lung. A modified Fick principle was used to calculate native cardiac output.

## RESULTS



## CONCLUSION

A modified Fick principle may provide accurate estimates of native cardiac output, but lack precision in a setting of veno-arterial extracorporeal membrane oxygenation